Investigation of the Satellite Attitude Control System Performance Using as Actuator Reaction Wheels

Souza[1,2], L C G , Fonseca[2], J B S

1) Brasilia University – UnB
Área Especial de Indústria-A-UnB, 72444-240, Brasília - DF- Brasil.
E-mail: lcgs@unb.br
2) National Institute for Space Research- INPE
Avenida dos Astronautas, 1758, São Jose dos Campos – SP – Brasil
E-mail: luiz.souza@.inpe.br, jesusbravo85@yahoo.com.br

SUMMARY: Satellite Attitude Control System (SACS) pointing accuracy is dependent of its actuator and sensor performance and robustness, where the first design requirement can be associated with bandwidth while the second is related to the ability of SACS to keep performance in face of system parameters variation. One way to gain attitude control algorithms confidence is through the conjunction of computational methods and experimental design, which allows hardware and software interface test, besides decreasing the SACS design cost. As for maneuver pointing accuracy the reaction wheel (RW) is a key actuator, because its disturbance can influence the accuracy and stability of SACS. This paper studies how the dynamics and the control algorithm strategy of the reaction wheels with its respective DC motor can influence the performance and robustness of the SACS control in three axes. To do this one develops a 3D satellite simulator nonlinear model based on the State-Dependent Riccati Equation (SDRE) method taking into account the RW parameters. One compares the performance and robustness of the SACS where the RW is commanded by the SDRE control law with algorithm based on current and speed feedback compensation. Simulations of the computational methods developed have shown that the RW with speed feedback compensation has improved the SACS performance and robustness.

KEYWORDS: satellite attitude control, reaction wheel.

1. INTRODUCTION

The design of a SACS, that involves plant uncertainties and large angle maneuvers followed by stringent pointing control, may require new nonlinear attitude control techniques in order to have adequate stability, good performance and robustness. Experimental SACS design using nonlinear control techniques through prototypes is one way to increase confidence in the control algorithm. Experimental design has the important advantage of representing the satellite dynamics in a laboratory setting, from which it is possible to accomplish different simulations to evaluate the SACS [1]. However, the drawback of experimental testing is the difficulty of reproducing zero gravity and torque free space conditions. A Multi-objective approach [2] has been used to design a satellite controller with real codification. An investigated through experimental procedure has been used by Conti and Souza in [3] for simulator inertia parameters identification. An algorithm based on the least squares method to identify mass parameters of a rotating space vehicle during attitude maneuvers has been developed by Lee and Wertz in [4]. The H-infinity control technique was used in [5] to design robust control laws for a satellite composed of rigid and flexible panels. In the SDRE method, the nonlinear dynamics are brought to a time-invariant, linear-like structure containing state-dependent coefficients. Infinite-horizon LQR is then applied to the linear-like structure with the coefficient matrices being evaluated at the current operational point in the state space. The process is repeated in the next sampling periods therefore producing and controlling several state dependent linear models out of a non-linear one. The SDRE method was applied in [6] for controlling a nonlinear rotatory flexible beam system with two-degrees of freedom. However, it did not incorporate the SDRE filter (Kalman filter) as a state observer for the SDRE method, so that uncertainties could be accounted for in the filtering process. This paper studies how the dynamics and the control algorithm strategy of the reaction wheels with its respective DC motor can influence the performance and robustness of the SACS control in three axes. To do this one develops a 3D satellite simulator nonlinear model based on the State-Dependent Riccati Equation (SDRE) method taking into account the RW largest possible number of variables. One compares the performance and robustness of the SACS where the RW is commanded by the SDRE control law with algorithm based on current and speed feedback compensation. Simulations results have shown that the RW with speed feedback compensation has improved the SACS performance and robustness. As a result, the simulations has shown the computational feasibility for real time implementation of the SDRE control method based on speed feedback algorithm in satellite´s onboard computer.

2. SDRE CONTROL METHODOLOGY

The Linear Quadratic Regulation (LQR) approach is well known and its theory has been extended for the synthesis of nonlinear control laws for nonlinear systems [7]. This is the case for satellite dynamics that are inherently nonlinear. A number of methodologies exist for the control design and synthesis of these highly nonlinear systems; these techniques include a large number of linear design methodologies such as Jacobean linearization and feedback linearization used in conjunction with gain scheduling [8]. Nonlinear design techniques have also been proposed including dynamic inversion and sliding mode control, recursive back stepping and adaptive control [9].

Compared to multi-objective optimization nonlinear control methods the SDRE method has the advantage of avoiding intensive interaction calculations, resulting in simpler control algorithms that are more appropriate for implementation on a satellite´s onboard computer.

The Nonlinear Regulator problem for a system represented in the State-Dependent Riccati Equation form with infinite horizon, can be formulated by minimizing the cost functional given by

$$J(x_0,u) = \frac{1}{2}\int_{t_0}^{\infty}(x^T Q(x)x+u^T R(x)u\,)dt \tag{1}$$

with the state $x \in \Re^n$ and control $u \in \Re^m$ subject to the nonlinear system constraints given by

$$\begin{aligned}\dot{x} &= f(x) + B(x)u\\ y &= C(x)x\\ x(0) &= x_0\end{aligned} \tag{2}$$

where $B \in \Re^{nxm}$ and C are the system input and the output matrices, and $y \in \Re^s$ ($\Re^s$ is the dimension of the output vector of the system). The vector initial conditions is x(0), $Q(x) \in \Re^{nxn}$ and $R(x) \in \Re^{mxm}$ are the weight matrix semi defined positive and defined positive.

Applying a direct parameterization to transform the nonlinear system into State Dependent Coefficients (SDC) representation, the dynamic equations of the system with control can be write in the form

$$\dot{x} = A(x)x + B(x)u \tag{3}$$

with $f(x) = A(x)x$, where $A \in \Re^{nxn}$ is the state matrix. By and large $A(x)$ is not unique. In fact there are an infinite number of parameterizations for SDC representation. This is true provided there are at least two parameterizations for all $0 \le \alpha \le 1$ satisfying

$$\alpha A_1(x)x + (1-\alpha)A_2(x)x = \alpha f(x) + (1-\alpha)f(x) = f(x) \tag{4}$$

The choice of parameterizations to be made must be appropriate in accordance with the control system of interest. An important factor for this choice is not violating the controllability of the system, i.e., the matrix controllability state dependent $[B(x) + A(x)B(x) \ldots A^{n-1}(x)B(x)]$ must be full rank.

The state-dependent algebraic Riccati equation (SDARE) can be obtained applying the conditions for optimality of the variational calculus. As a result, the Hamiltonian for the optimal control problem given by Equations (1) and (2) is given by

$$H(x,u,\lambda) = \frac{1}{2}(x^T Q(x)x + u^T R(x)u\,) + \lambda^T(A(x)x + B(x)u) \tag{5}$$

where $\lambda \in \Re^n$ is the Lagrange multiplier.

Applying to the Eq.(5) the necessary conditions for the optimal control given by $\dot{x} = \frac{\partial \boldsymbol{H}}{\partial \lambda}$, $\frac{\partial \boldsymbol{H}}{\partial u} = 0$ and $\dot{\lambda} = -\frac{\partial \boldsymbol{H}}{\partial x}$, one gets

$$\dot{\lambda} = -Q(x)x - \frac{1}{2}x^T\frac{\partial Q(x)}{\partial x}x - \frac{1}{2}u^T\frac{\partial R(x)}{\partial x}u - \left[\frac{\partial(A(x)x)}{\partial x}\right]^T\lambda - \left[\frac{\partial(B(x)u)}{\partial x}\right]^T\lambda \tag{6}$$

$$\dot{x} = A(x)x + B(x)u \tag{7}$$

$$0 = R(x)u + B(x)\lambda \tag{8}$$

Assuming the co-state in the form λ=P(x)x, which is dependent of the state, from Eq.(8) one obtains the feedback control law

$$u = -R^{-1}(x)B^T(x)P(x)x \tag{9}$$

Substituting this result into Eq. (7) one gets

$$\dot{x} = A(x)x - B(x)R^{-1}(x)B^T(x)P(x)x \tag{10}$$

To find the function P (x) one differentiates λ = P (x) with respect the time along the path from which one gets

$$\dot{\lambda} = \dot{P}(x)x + P(x)\dot{x} = \dot{P}(x)x + P(x)A(x)x - P(x)B(x)R^{-1}(x)B^T(x)P(x)x \tag{11}$$

Substituting Eq.(11) in the first necessary condition of optimal control (Eq.6) one obtains

$$\begin{aligned}&\dot{P}(x)x + P(x)A(x)x - P(x)B(x)R^{-1}(x)B^T(x)P(x)x\\ &= -Q(x)x - \frac{1}{2}x^T\frac{\partial Q(x)}{\partial x}x - \frac{1}{2}u^T\frac{\partial R(x)}{\partial x}u - \left[A(x) + \frac{\partial(A(x)x)}{\partial x}x\right]^T P(x)x\\ &- \left[\frac{\partial(B(x)u)}{\partial x}\right]^T P(x)x\end{aligned} \tag{12}$$

Arranging the terms more appropriately one has

$$\begin{aligned}&\dot{P}(x)x + \frac{1}{2}x^T\frac{\partial Q(x)}{\partial x}x + \frac{1}{2}u^T\frac{\partial R(x)}{\partial x}u + x^T\left[\frac{\partial\big(A(x)\big)}{\partial x}\right]^T P(x)x + \left[\frac{\partial(B(x)u)}{\partial x}\right]^T P(x)\\ &+ [\,P(x)A(x) + A^T(x)P(x) - P(x)B(x)R^{-1}(x)B^T(x)P(x) + Q(x)]x\\ &= \;\; 0\end{aligned} \tag{13}$$

In order to satisfy the equality of Eq.(13) one obtains two important relations. The first one is state-dependent algebraic Riccati equation (SDARE) which solution is P(x) given by

$$P(x)A(x) + A^T(x)P(x) - P(x)B(x)R^{-1}(x)B^T(x)P(x) + Q(x) = 0 \tag{14}$$

The second one is the necessary condition of optimality which must be satisfied and it is given by

$$\begin{aligned}&\dot{P}(x)x + \frac{1}{2}x^T\frac{\partial Q(x)}{\partial x}x + \frac{1}{2}u^T\frac{\partial R(x)}{\partial x}u + x^T\left[\frac{\partial\big(A(x)\big)}{\partial x}\right]^T P(x)x + \left[\frac{\partial(B(x)u)}{\partial x}\right]^T P(x)x\\ &= 0\end{aligned} \tag{15}$$

For the infinite time problem and considering the standard Linear Quadratic Regulator (LQR) problem, this is a condition that satisfies the optimality of the solution suboptimal control.
Finally, the nonlinear control law fed back by the states has the following form

$$u = -S(x)x\,,\;\; with\;\; S(x) = R^{-1}(x)B^T(x)P(x) \tag{16}$$

For some special cases, such as systems with little dependence on the state or with few state variables, Eq. (14) can be solved analytically. On the other hand, for more complex systems the numerical solution can be obtained using an adequate sampling rate. It is assumed that the parameterization of the coefficients dependent on the state is chosen so that the pair (A(x), B(x)) and (C(x) , A(x)) are in the linear sense for all x belonging to the neighborhood about the origin, point to point, stabilizable and detectable, respectively. Similar to the LQR method the SDRE nonlinear regulator need that all states are available to be feedback, otherwise one has to use the Kalman filter to estimates the data that is not measurable.

3. SIMULATOR MODEL

Figure 1 shows the INPE 3-D simulator which has a disk-shaped platform, supported on a plane with a spherical air bearing. Considering that the INPE 3-D simulator is not complete build, one assumes that there are three reaction wheel configuration set capable to perform maneuver around the three axes and that there are three angular velocities sensor, like gyros. Apart from the difficulty of reproducing zero gravity and torque free condition, modeling a 3-D simulator, basically, follows the same step of modeling a rigid satellite with rotation in three axes free in space.

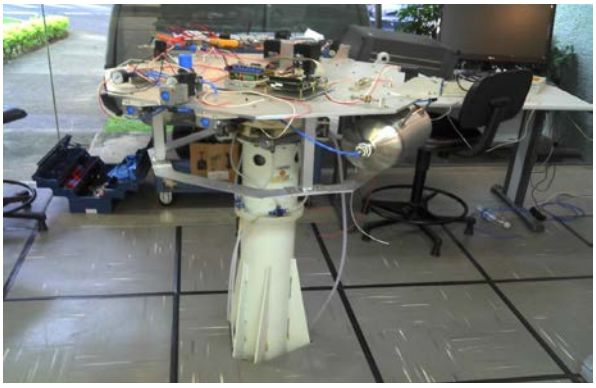

Figure 1- INPE 3-D simulator three reaction wheels.

The orientation of the platform is given by the body reference system F_b with respect to inertial reference system F_I considering the principal axes of inertia and using the Euler angles (θ_1, θ_2, θ_3) in the sequence 3-2-1, to guarantee that there is no singularity in the simulator attitude rotation. The equations of motions are obtained using Euler´s angular moment theorem given by

$$\dot{\vec{h}} = \vec{g} \tag{17}$$

where $\vec{g}$ and $\vec{h}$ are the torque and the angular moment of the system, which is given by

$$\vec{h} = I\vec{\omega} + I_w\left(\vec{\Omega} + \vec{\omega}\right) \tag{18}$$

where I = diag (I_{11}, I_{22}, I_{33}) is the system matrix inertia moment, $\vec{\omega}$ is the angular velocity of the platform, $\vec{I}_w$ = diag (I_{w1}, I_{w2}, I_{w3}) is the reaction wheel matrix inertia moment and Ω = (Ω_1, Ω_2, Ω_3) are the reaction wheel angular velocity.

Differentiating Eq. (18) and considering that the angular velocity of F_b is $\vec{\omega}$ and that the external torque is equal to zero, one has

$$\dot{\vec{h}} + \vec{\omega}^x \vec{h} = 0 \tag{19}$$

Substituting Eq.(18) into Eq.(19), the acceleration of the system is

$$\dot{\vec{\omega}} = \left(I + I_w\right)^{-1}\left[-\vec{\omega}^x\left(I + I_w\right)\vec{\omega} - \vec{\omega}^x I_w \vec{\Omega} - I_w \dot{\vec{\Omega}}\right] \tag{20}$$

The simulator attitude as function of the angular velocity is

$$\begin{pmatrix} \dot{\theta}_1 \\ \dot{\theta}_2 \\ \dot{\theta}_3 \end{pmatrix} = \begin{pmatrix} 0 & \sin\theta_3/\cos\theta_2 & \cos\theta_3/\cos\theta_2 \\ 0 & \cos\theta_3 & -\sin\theta_3 \\ 1 & \sin\theta_3\sin\theta_2/\cos\theta_2 & \cos\theta_3\sin\theta_2/\cos\theta_2 \end{pmatrix} \begin{pmatrix} \omega_1 \\ \omega_2 \\ \omega_3 \end{pmatrix} \tag{21}$$

Here one simulates the angular maneuver which represents the fine pointing mode control where the reaction wheel is the best actuator, so the state's x are $(\theta_1\ \theta_2\ \theta_3\ \omega_1\ \omega_2\ \omega_3)^T$ and the control are due to the reaction wheel velocities $(\dot{\Omega}_1\ \dot{\Omega}_2\ \dot{\Omega}_3)^T$ One knows that the reaction wheel generates internal torques and the attitude control is performed by exchange of angular moment between the reaction wheel and the satellite. From the union of the Equations (20) and (21) one obtains the matrices A(x), B(x) and C(x) in state space form, which represents the satellite simulator nonlinear plant (yellow block) as showed in Figure 5. It should be stressed, that a great advantage of the SDRE method is that it is not necessary to linearize the system. The SDRE method can deal with the nonlinearities of the system, which here come from the product of the angular velocities of the platform and reaction wheel (Eq.(20)) and with the trigonometric function of Eq.(21) associated with the angular position that represent the attitude of the system.

4. REACTION WHEEL DYNAMICS

In the sequel one derives the reaction wheel dynamics which is triggered by a DC motor as show in Figure 2. For simplicity, here one ignores the losses due to the transformation of electrical energy into mechanical. Therefore, the electrical power is equal to the mechanical power given by

$$V(t)i(t) = T(t)w(t) \tag{22}$$

$$V(t) = Ri(t) + L\frac{di(t)}{dt} + e(t) \tag{23}$$

$$T(t) = Bw(t) + j\frac{dw(t)}{dt} \tag{24}$$

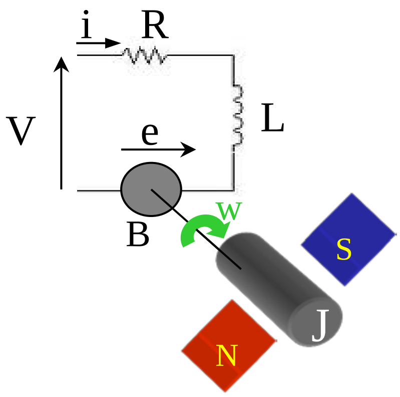

Figure 2- DC Motor dynamics representation**.**

Where R is the electrical resistance of the motor, L is the inductance of the motor, B is the viscous friction of the motor, J is the moment of inertia of the reaction wheel, w is the angular velocity of the wheel, i is the electric current of the motor, V is the electrical voltage at the motor terminals and e is the voltage generated due to movement of the motor rotor within a magnetic flux.
For a permanent magnet motor, the following relationship given below is valid

$$e(t) = K_e w(t) \tag{25}$$

where K_e is associated with the motor tension. One also knows that in an engine of this type the relationship between torque and current is given by

$$T(t) = K_t i(t) \tag{26}$$

where Kt is a constant associated with the motor torque. Substituting Eq. (25) into Eq. (23) one has

$$V(t) = Ri(t) + L\frac{di(t)}{dt} + k_e w(t) \tag{27}$$

Substituting Equation (26) into Equation (24) one has

$$K_t i(t) = Bw(t) + j\frac{dw(t)}{dt} \tag{28}$$

Arranging the Equations (27) and (28) with the first order terms in the left hand side and the zero order terms in the right hand one has

$$L\frac{di}{dt} = V - Ri - K_e w \tag{29}$$

$$j\frac{dw}{dt} = K_t\, i - Bw \tag{30}$$

Putting Equations (29) and (30) in the Matlab/Simulink form, one has the block diagram given by Figures 3 and 4, respectively.

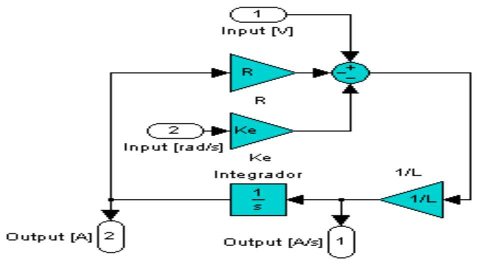

Figure 3 - block diagram of Eq. (29)

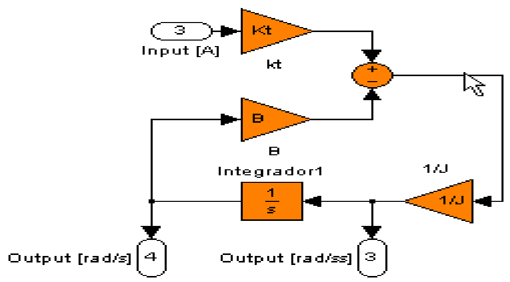

Figure 4 - block diagram of Eq. (30)

Joining the two block diagrams of the Figures 3 and 4 above, one gets the complete block diagram of the entire reaction wheel (blue bock) as showed in Figure 5.

5. SIMULATIONS RESULTS

Now one has the Simulink/Matlab model for the Satellite Simulator with Nonlinear Plant (yellow block), the control system using the SDRE Controller (green block) and the reaction wheel dynamics with velocity or current feedback (blue block), so grouping them one gets the Complete Simulator System , showed in Figure 5. In such system one has as input the reference angles to where the SDRE controller must maneuver the satellite and as output the angles and the angular velocity of the satellite. For simplicity the external torque is zero.

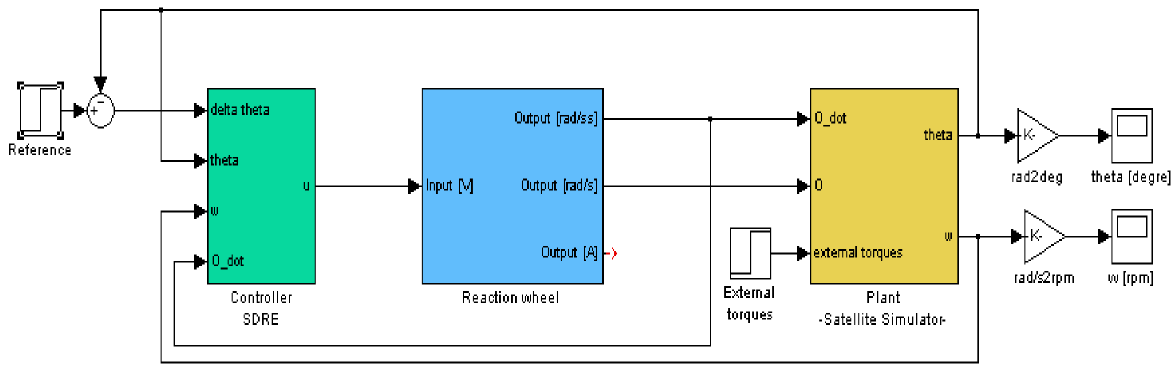

Figure 5 – Entire Simulator with plant of the satellite, SDRE Controller and the Reaction Wheel dynamics.

The satellite simulator model is inertia moment depend, so here one uses $I_{11} = I_{22}$=1185.0; I_{33}=1136.0 and for the DC motors parameters R = 7,3 , L = 2,5 , B = 0,00494, J = 2.0, Kt = 0,05, Ke = 0,05. The SDRE controller must maneuver the satellite from initial angles zeroes to final angles are Theta1 = 10°, Theta2 = 5°, Theta3 = - 5°. The control system has used three different reaction wheel configurations. In the first one the reaction wheel has no feedback, in the second and thirty configurations one employs velocity feedback and current feedback, as showed in Figure 6, in order to evaluate the reaction wheel performance for the three cases.

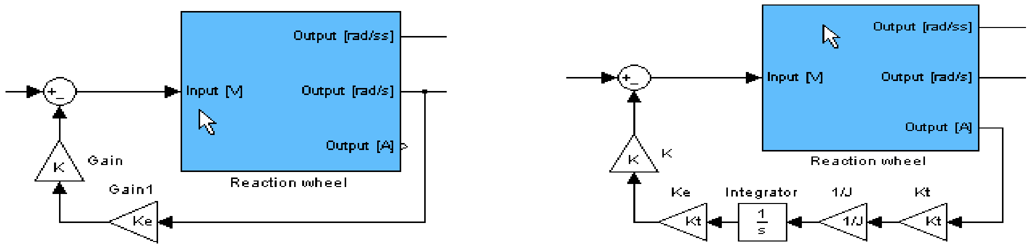

Figure 6 – reaction wheel block diagram with velocity and current feedback

The first simulation is the design of the SDRE controller where the reaction wheel loop has no feedback. The SDRE controller gain S(x) depend on matrices of the simulator model A(x), B(x) and C(x), see [16] for details, and of the tuning matrices Q and R which one assumes the values Q = diag(1, 1, 1,100, 100, 100) and R (0.001, 0.001,0.011). Once one has design the SDRE controller the next step is to design the reaction wheel control loop which can have velocity or current feedback. After some try and error one get the gain K = 50 to feedback with velocity or current the reaction wheel. The performance of the entire SACS for the previously angular maneuver is showed in Figures 7, 8 and 9 for each axis angles Theta1, 2 and 3, without feedback and with feedback of velocity and current, respectively

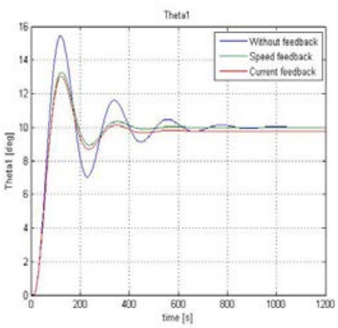

Figure 7 – Attitude angle Theta 1

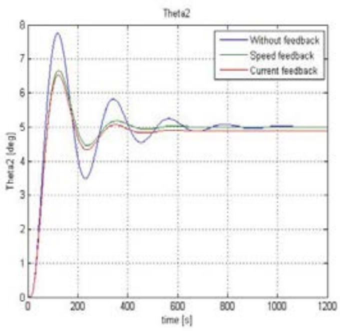

Figure 8 – Attitude angle Theta 2

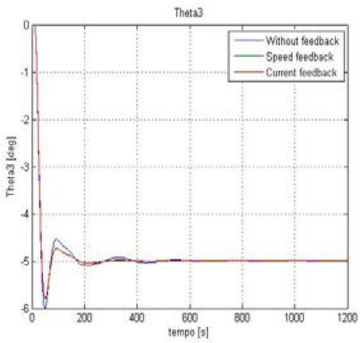

Figure 9 – Attitude angle Theta 3

In order to investigate the reaction wheel performance one increases its gain to K= 250 and perform the same previously angular maneuver. Figures 10, 11 and 12 show the SACS action for each angle Theta1, 2 and 3, without feedback and with feedback of velocity and current, respectively

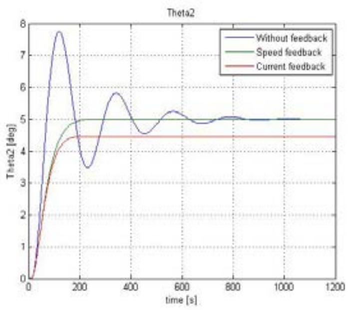

Figure 10 – Attitude angle Theta 1

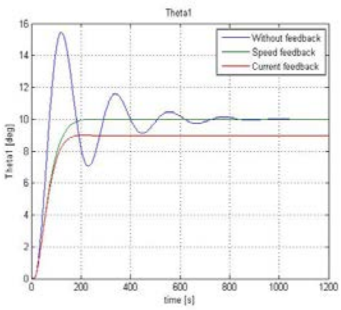

Figure 11 – Attitude angle Theta 2

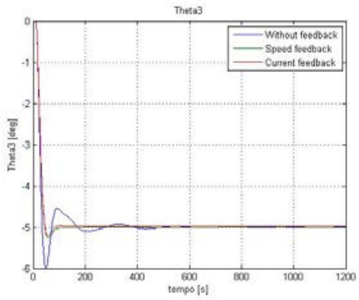

Figure 12 – Attitude angle Theta 3

As one observes the SACS performance has been improved when the reaction wheel gain increases, so one increases it a bit more to K= 500 and one performs the same angular maneuver. Figures 13, 14 and 15 show that the SACS performance to control the angles Theta1, 2 and 3 has been deteriorated both with velocity and current feedback.

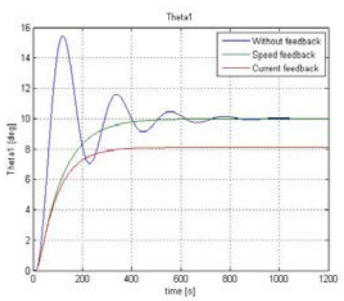

Figure 13 – Attitude angle Theta 1

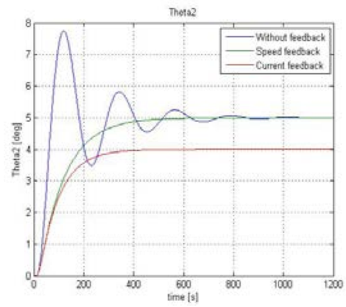

Figure 14 – Attitude angle Theta 2

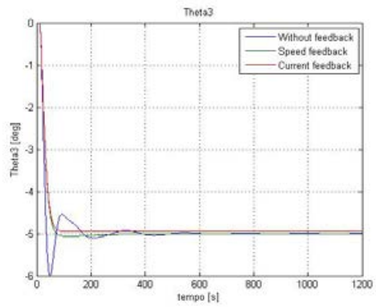

Figure 15 – Attitude angle Theta 3

4. CONCLUSIONS

From the first simulation one observes that the SACS with reaction wheel loop using the gain *K*=50 has better performance than the SACS with reaction wheel without both velocity or current feedback, since there is an improvement in the level of the overshoot and the maneuver has been done faster, although one observes that there is a stead state error when using the current feedback. So one can conclude that increasing the reaction wheel gain the velocity feedback has better performance that current feedback. In order to investigate this and to improve the maneuver one has increase the reaction wheel loop gain to *K* = 250, in that case one notices that stead state error introduced by the current feedback increase, although the overshoot has decreased. As a result, one could conclude that increasing the reaction wheel gain the SACS performance using the velocity feedback in the reaction wheel loop could be better than current. But this is not true since when one increase a bit more the gain to *K* = 500, the maneuver using the reaction wheel with velocity feedback has been performed in more time than the maneuver using *K*= 250. This just shows that there exists a limit value for the reaction wheel gain which possible is around 250. Besides, it is important to say that the reaction wheel gain is as function of its axis since the inertia moments are different for each axis. Finally, one observes that there are two ways to improve the SACS design, the first one could be using a kind of optimal control technique to obtain the reaction wheel gains, and the other one is including a Kalman filter to estimate the possible measurements that eventually are not available to be feedback, since here one has consider that all states are available to be feedback into the control loop.

5. REFERENCES

[1] Hall, C.D., Tsiotras and Shen, H. “Tracking Rigid Body Motion Using Thrusters and Momentum Wheels”. *Journal of the Astronautical Sciences.* (3), 2002, pp. 13-20.

[2] Mainenti-Lopes, I. , Souza, L. C. G., Sousa, F. L., Cuco, A. P. C. “ Multi-objective Generalized Extremal Optimization with real codification and its application in satellite attitude control”, Proceedings of 19th International Congress of Mechanical Engineering - COBEM, Gramado, 2009, Brasil.

[3] Conti, G T and Souza, L C G. “Satellite Attitude System Simulator”, *Journal of Sound and Vibration*,(15), 2008, pp. 392-395.

[4] Lee, A. Y. and Wertz, J. A. “In-flight estimation of the Cassini Spacecraft inertia tensor”. Journal Spacecraft, (39),1, 2002, pp.153-155.

[5] Pinheiro, E. R.; Souza, L. C. G**.**. Design of the Microsatellite Attitude Control System Using the Mixed H2/Hoo Method via LMI Optimization. Mathematical Problems in Engineering, v. 2013, p. 1-8, 2013.

[6] Bigot, P., Souza, L. C. (2014). Investigation of the State Dependent Riccati Equation (SDRE) adaptive control advantages for controlling non-linear systems as a flexible rotatory beam. *International journal of systems applications, engineering and development*. (Vol. 8, pp 92-99).

[7] Menon P.K. ; Lam T. ; Crawford L. S.; Cheng V. H L, “Real Time Computational Methods for SDRE Non-linear Control of Missiles”. *American Control Conference*, May 8-10, 2002, Anchorage, AK, USA.

[8] Shamma, J. S. and Athens, M. Analysis of gain scheduled control for nonlinear plants. IEEE Trans. on Auto. Control, 35(8):898{907, 1990.

[9] Slotine, J. J. E.. Applied nonlinear control. Prentice Hall, Englewood Clips, New Jersey, 1991.